

Standard Model Predictions for CP Violation in B^0 Meson Decay^{*}

CLAUDIO O. DIB,[†] ISARD DUNIETZ, FREDERICK J. GILMAN, AND YOSEF NIR

*Stanford Linear Accelerator Center
Stanford University, Stanford, California 94309*

ABSTRACT

We examine the present set of constraints on the parameters of the Standard Model and use the unitarity triangle to present their allowed range. We give the implications of this for CP violation in the B meson system as a function of top quark mass, emphasizing what luminosity of an electron-positron collider is needed to guarantee a statistically significant asymmetry in one or more B decay channels.

Submitted to *Physical Review D*

^{*} Work supported by the Department of Energy, contract DE-AC03-76SF00515.

[†] Now at Department of Physics, University of California, Los Angeles, CA 90024.

1. Introduction

Even though twenty-five years have passed since the discovery¹ of CP violation, its observation only within the K meson system has left us with different hypotheses as to its origin. However, during that time the Standard Model of the electroweak interactions has been developed, in which CP violation has a natural place, the Cabibbo–Kobayashi–Maskawa (CKM) mixing matrix:

$$V = \begin{pmatrix} V_{ud} & V_{us} & V_{ub} \\ V_{cd} & V_{cs} & V_{cb} \\ V_{td} & V_{ts} & V_{tb} \end{pmatrix}. \quad (1.1)$$

A unique CP-violating phase could occur with three generations of quarks. Independent of any phase convention in defining the matrix, the phase could be taken to be

$$\arg(V_{us}V_{ub}^*V_{cs}^*V_{cb}). \quad (1.2)$$

The question before us is whether this is indeed the origin of CP violation as it is observed in nature. If this phase were to explain what is observed in K decays, then large CP-violating asymmetries would be predicted in neutral B meson decays.

This report presents the current status of what can be said about such asymmetries in the context of our knowledge of the experimental constraints on the parameters of the Standard Model, updating and extending previous work.^{2–5} We use the unitarity triangle of the CKM matrix to show these constraints as a function of top quark mass. The CP-violating asymmetries for neutral B meson decays in which we are interested are related to the angles of the unitarity triangle. The consequent range of asymmetries allowed for a given type of B decay is evaluated, and the luminosity of an electron-positron collider needed in order to guarantee

a statistically significant measurement of CP violation in one or more types of B decay is then presented.

2. The Unitarity Triangle

Unitarity of the 3×3 CKM matrix yields

$$V_{ud} V_{ub}^* + V_{cd} V_{cb}^* + V_{td} V_{tb}^* = 0. \quad (2.1)$$

The unitarity triangle is just a geometrical presentation of this equation in the complex plane.⁶ We can always choose to orient the triangle so that $V_{cd} V_{cb}^*$ lies along the horizontal axis. This is equivalent to choosing a phase convention. In any case, the parametrization adopted by the Particle Data Group⁷ makes V_{cb} real and V_{cd} real to a very good approximation. Also, $V_{ud} \approx 1$, $V_{tb} \approx 1$, and $V_{cd} \approx -\sin \theta_C = -0.22$, and Eq. (2.1) now becomes

$$V_{ub}^* + V_{td} = |V_{cd} V_{cb}|, \quad (2.2)$$

which is shown as the unitarity triangle in Figure 1.

CP-violating asymmetries between B^0 and \bar{B}^0 mesons decaying to CP eigenstates are proportional to $\sin(2\phi)$, where ϕ stands for one of the angles (labelled α , β , and γ in Figure 1) of the triangle.⁸ Rescaling the triangle by $[1/(|V_{cd} V_{cb}|)]$, the coordinates of the three vertices A , B , and C become:

$$A\left(\frac{\text{Re}V_{ub}}{|V_{cd} V_{cb}|}, -\frac{\text{Im}V_{ub}}{|V_{cd} V_{cb}|}\right); \quad B(1, 0); \quad C(0, 0). \quad (2.3)$$

In the Wolfenstein parametrization,⁹ which is just the small mixing-angle approximation given here with the matrix elements expressed in terms of powers of $\sin \theta_C$,

the coordinates of the vertex A are (ρ, η) . What remains for Section 4 is to constrain the point A by using the experimental data which are presently available.

3. CP Violation with Neutral B Mesons

The decay rate of a time-evolved, initially pure B^0 (\bar{B}^0) into a CP-eigenstate, f , is:¹⁰

$$\begin{aligned}\Gamma(B_{\text{phys}}^0(t) \rightarrow f) &\propto e^{-\Gamma t} [1 - \text{Im } \lambda \sin(\Delta m t)] \\ \Gamma(\bar{B}_{\text{phys}}^0(t) \rightarrow f) &\propto e^{-\Gamma t} [1 + \text{Im } \lambda \sin(\Delta m t)].\end{aligned}\tag{3.1}$$

CP-violating effects are manifest through the presence of the interference term $\text{Im } \lambda$. For the processes under consideration here, the CP violation arises from the quantum mechanical interference of amplitudes corresponding to two paths to the same final state, one of which involves $B^0 - \bar{B}^0$ mixing. Possible small CP-violating effects in the decay amplitude itself are neglected. Care must be taken whether the final state is CP-even or odd, since that flips the sign of the interference term:¹¹ $\text{Im } \lambda_{\text{odd}} = -\text{Im } \lambda_{\text{even}}$. We always quote the interference terms obtained for CP-even eigenstates.

For a given *quark* subprocess, Table 1 lists a few corresponding *hadronic* final states and the relevant interference term, $\text{Im } \lambda$, responsible for CP-violation (stated in terms of the angles in the unitarity triangle).

TABLE 1

Decay Modes and Interference Terms for Various Classes

Quark sub-process (class)	Decay mode	Im λ
$\bar{b} \rightarrow \bar{c} + c\bar{s}, \bar{c} + c\bar{d}, \bar{s}$ (i)	$B_d \rightarrow \psi K_S, \chi K_S, \phi K_S, \eta_c K_S,$ $\omega K_S, \rho K_S, D^+ D^-, \bar{D}^0 D^0,$ $\psi K_L, \phi K_L, \rho K_L, \dots$	$-\sin(2\beta)$
$\bar{b} \rightarrow \bar{u} + u\bar{d}$ (ii)	$B_d \rightarrow \pi^+ \pi^-, \bar{p}p, \rho\pi^0,$ $\omega\pi^0, \pi^0\pi^0$	$-\sin(2\alpha)$
$\bar{b} \rightarrow \bar{u} + u\bar{d}$ (iii)	$B_s \rightarrow \rho K_S, \omega K_S,$ $\rho K_L, \omega K_L$	$-\sin(2\gamma)$
$\bar{b} \rightarrow \bar{c} + c\bar{s}, \bar{c} + c\bar{d}$	$B_s \rightarrow \psi\phi, \eta_c\phi, \psi K_S$	$2 \left \frac{V_{us} V_{ub}}{V_{ud} V_{cb}} \right \sin \gamma$

We concentrate on three promising classes of measurements:

(i) Measuring $\sin(2\beta)$ in B_d decays:

This class has the advantage that different quark subprocesses: $\bar{b} \rightarrow \bar{c} + c\bar{s}, \bar{b} \rightarrow \bar{c} + c\bar{d}, \bar{b} \rightarrow \bar{s}$, all yield the same interference term,¹² $\text{Im } \lambda = -\sin(2\beta)$. The standard example at the hadron level is $B_d \rightarrow \psi K_S$, with an observed¹³ $BR(B_d \rightarrow \psi K_S) \approx 3 \times 10^{-4}$. To increase statistics, one can look at many decay modes: $B_d \rightarrow \chi K_S, \phi K_S, \rho K_S, \omega K_S, D^+ D^-, \bar{D}^0 D^0, \psi K_L, \phi K_L, \rho K_L$, etc.

(ii) Measuring $\sin(2\alpha)$ in B_d decays:

The relevant quark subprocess here is $\bar{b} \rightarrow \bar{u} + u\bar{d}$. Possible two-body hadronic decay modes are¹⁴ $B_d \rightarrow \pi^+ \pi^-, \omega\pi^0, \rho\pi^0$, and $B_d \rightarrow \bar{p}p$. These modes may suffer from additional contributions, either from virtual intermediate states,

in the form of penguin diagrams at the quark level,^{15,16} or from real intermediate states, *i.e.*, rescattering effects at the hadron level. For example,¹⁷ $B_d \rightarrow D^+ D^- \rightarrow \pi^+ \pi^-$ may upset the identification of $B_d \rightarrow \pi^+ \pi^-$ as a pure $\bar{b} \rightarrow \bar{u} + u\bar{d}$ transition. Although difficult to calculate quantitatively, a recent estimate¹⁵ is that these additional contributions are less than a 20% effect for class (ii) decays, and they will be neglected here. In addition, the mode $p\bar{p}$ has opposite CP-parity in the s- and p-wave final states, producing asymmetries of opposite sign.

(iii) Measuring $\sin(2\gamma)$ in B_s decays:

The relevant quark subprocess is, $\bar{b} \rightarrow \bar{u} + u\bar{d}$, the same as that in class (ii). However, $\text{Im } \lambda$ is related to a different angle of the unitarity triangle, because the interference term depends not only on the quark subprocess but on $B^0 - \bar{B}^0$ mixing, which in turn involves different CKM elements for the B_d and B_s systems. Possible hadronic modes of this type are $B_s \rightarrow \rho K_S$ and $B_s \rightarrow \omega K_S$, although again rescattering effects may be important.¹⁷

A fourth class utilizes the quark subprocesses in class (i), but for B_s rather than B_d decays. The predicted interference term is very small, at most of order $\sin^2 \theta_C \sin \gamma$.

In addition to the three promising classes above, decays to CP non-eigenstates could also show large CP-violating effects, but they are not susceptible to the same clean interpretation in terms of just CKM matrix elements. This report will be restricted to the predicted CP asymmetries in classes (i) – (iii) only.

4. Constraining the Unitarity Triangle

Now that the relevance of various B -decay asymmetries has been presented, we return to the unitarity triangle and the measurements which we will use to constrain it. Two of these constraints depend on loop processes: the CP-violating parameter ϵ and the $B_d - \bar{B}_d$ mixing parameter x_d . As loop processes are GIM-suppressed, the resulting constraints strongly depend on the yet-unknown mass of the top quark, m_t . The detailed analytical expressions may be found elsewhere.¹⁸ On the other hand, $|V_{cb}|$ and $|V_{ub}/V_{cb}|$ are directly measurable in semileptonic B decay, and thus independent of m_t .

The values of well-known quantities used here are:

$$\begin{aligned}
 f_K &= 0.16 \text{ GeV}; \quad m_c = 1.4 \text{ GeV}; \quad m_B = 5.28 \text{ GeV}; \quad M_W = 80 \text{ GeV}; \\
 G_F &= 1.166 \times 10^{-5} \text{ GeV}^{-2}; \quad |V_{us}| = \sin \theta_C = 0.22; \quad |\epsilon| = 2.26 \times 10^{-3}.
 \end{aligned}
 \tag{4.1}$$

The QCD correction factors for ϵ and x_d are the same as those used in Ref. 18. We consider the ranges⁷

$$0.036 \leq |V_{cb}| \leq 0.056, \tag{4.2}$$

and^{19,20} $78 \text{ GeV} \leq m_t \leq 200 \text{ GeV}$. The constraints on the rescaled unitarity triangle are then imposed as follows:

- a. The top mass is fixed within the range given above. As examples we choose $m_t = 80, 120, 160,$ and 200 GeV in Figures 2, 3, 4, and 5, respectively.
- b. The value of $|V_{cb}|$ is fixed within the range given above. As examples we choose $|V_{cb}| = 0.036, 0.046,$ and 0.056 in subfigures a, b, and c, respectively.

c. The constraint²¹

$$0.04 \leq |V_{ub}/V_{cb}| \leq 0.16. \quad (4.3)$$

is imposed. This forces the vertex A to lie between two circles centered at the vertex $C(0,0)$. In the Figures, those circles are dotted.

d. The x_d constraint is imposed. This requires the vertex A to lie between two circles (dashed in the Figures) centered at $B(1,0)$. The width of this band arises mainly from theoretical uncertainties in $B_B f_B^2$ and, to a lesser extent, from lifetime and mixing²¹ measurements:

$$\begin{aligned} (0.1 \text{ GeV})^2 &\leq B_B f_B^2 \leq (0.2 \text{ GeV})^2 \\ 1.04 \text{ ps} &\leq \tau_b \leq 1.32 \text{ ps} \\ 0.50 &\leq x_d \leq 0.78 . \end{aligned} \quad (4.4)$$

e. The ϵ -constraint is imposed. This demands that the vertex A lie between the two hyperbolas (solid curves in the Figures). The width of this band arises from the theoretical uncertainty in the B_K parameter:

$$1/3 \leq B_K \leq 1 . \quad (4.5)$$

The final allowed domain for the vertex A is given by the shaded region in Figures 2–5. We stress again that the $|V_{ub}/V_{cb}|$ constraint does not depend on either m_t or $|V_{cb}|$. In contrast, the ϵ and x_d constraints do change. Larger m_t or larger $|V_{cb}|$ values correspond to smaller radii for the x_d circles and, in general, to an ϵ band which is lower and narrower.

The allowed values for the angles α, β , and γ can be deduced from Figures 2–5. Figure 6 shows the minimum and maximum values for these angles as a function of

the top mass, where the parameters range according to Eqs. (4.1)–(4.5). *Note that a value of 45° corresponds to a maximal CP asymmetry, while 90° for an angle implies that there will be no CP asymmetry in the corresponding class of B decays. However, if one angle is 90° , then CP violation will necessarily exhibit itself in the other two classes.* Examining Figures 2–5, we see that either α or γ may be 90° when $m_t \gtrsim 80 \text{ GeV}$. Consequently, zero asymmetries may occur for class (ii), e.g., $B_d \rightarrow \pi^+\pi^-$, or class (iii), e.g., $B_s \rightarrow \rho K_S$ decays, respectively. In contrast, the angle β ranges between

$$2^\circ < \beta \leq \arcsin |V_{ub}/(V_{cd}V_{cb})| \approx 47^\circ . \quad (4.6)$$

Thus, the interference term for class (i), e.g., $B_d \rightarrow \psi K_S$ decays with $\text{Im } \lambda = -\sin(2\beta)$, is never zero, always negative, and can reach -1 .

5. Ranges of CP Asymmetries for B^0 Mesons

To estimate the number of $b\bar{b}$ events required to measure CP violation, it is crucial to calculate the allowed range for the interference terms, $\text{Im } \lambda$. The constraints of Eqs. (4.1)–(4.5) are employed. Figure 7 shows the minimum and maximum of $-\sin(2\phi)$ for $\phi = \alpha, \beta, \gamma$, as a function of the top mass. The dotted line displays the lower bound on the *absolute* value, $|\sin(2\phi)|$.

With $m_t \approx 50 \text{ GeV}$, large CP asymmetries in all three classes would be predicted (see Figure 7). A small top mass forces the vertex A to lie in a narrow allowed region with a large imaginary part η (due to the ϵ constraint) and with negative ρ values (due to the x_d constraint), as can be seen in Figure 2. With large top mass, the situation is very different. The allowed region becomes larger, and

all values for the interference term of classes (ii) and (iii) are allowed,

$$-1 \leq \{-\sin(2\alpha) \text{ or } -\sin(2\gamma)\} \leq 1. \quad (5.1)$$

The possibilities range from maximal ($|\text{Im } \lambda| = 1$) to vanishing ($|\text{Im } \lambda| = 0$) CP asymmetry.²²

The fact that a particular interference term might vanish is disconcerting; if we were “unlucky” in the shape of the unitarity triangle chosen by nature, the failure to observe CP violation in just a class (ii) or just a class (iii) process would not be evidence against CP violation originating in the CKM matrix. It is better to have a measurement for which a nonvanishing asymmetry is guaranteed. This is indeed the case for class (i) processes, since the angle β satisfies (see Figure 7b):

$$-1 \leq -\sin(2\beta) \lesssim -0.08. \quad (5.2)$$

Therefore, we are guaranteed that there are processes for which the magnitude of the CP-violating interference term, $|\text{Im } \lambda|$, is greater than about 0.08 and can even be maximal.²³ We define I_1 as the lower bound on $|\sin(2\beta)|$, and present it as a function of the top mass in Figure 8. Can we do better from the point of view of having at least one asymmetry which is bigger than I_1 ? The answer is certainly yes if we measure processes that reside in two or three different classes, and consider the biggest value of $|\sin(2\phi)|$ which corresponds to any of these classes.

To make this quantitative, we define the following quantities for any allowed unitarity triangle Δ :

$$\begin{aligned} \max_2(\Delta) &\equiv \max\{|\sin(2\alpha)|, |\sin(2\beta)|\} \\ \max_3(\Delta) &\equiv \max\{|\sin(2\alpha)|, |\sin(2\beta)|, |\sin(2\gamma)|\} \end{aligned} \quad (5.3)$$

If we now range over all allowed triangles, we define

$$\begin{aligned} I_2 &\equiv \min_{\text{all } \Delta} \{ \max_2(\Delta) \} \\ I_3 &\equiv \min_{\text{all } \Delta} \{ \max_3(\Delta) \} \end{aligned} \tag{5.4}$$

What is the significance of I_2 ? An experiment which is sensitive to *both class (i) and class (ii)* processes is assured that $|\text{Im } \lambda| \geq I_2$ for at least one of the two classes. Figure 8 shows I_2 plotted against the top mass. Small top masses (≈ 80 GeV), or large ones (≈ 200 GeV), have $I_2 > 0.2$. This situation would be encouraging for CP violation studies. In contrast, intermediate top masses (≈ 130 GeV) allow I_2 to be just above 0.1 .

Similarly, an experiment searching simultaneously for CP-asymmetries in processes of all three different classes is guaranteed to find that $|\text{Im } \lambda| \geq I_3$ for at least one of the three classes of CP-violating asymmetries. We present I_3 as a function of the top mass in Figure 8. Small top masses (≈ 80 GeV) or large ones (≈ 200 GeV) have $I_3 > 0.3$, and intermediate top masses (≈ 130 GeV) have a minimum value of I_3 just below 0.2 . An important conclusion is that there exists an angle $\phi = \alpha, \beta$, or γ such that $|\sin(2\phi)| \gtrsim 0.2$. *There must be substantial CP violation in at least one of the three classes if the Standard Model is the source of CP violation.*

Simple geometrical considerations lead to another point of interest. If there is a near-maximal interference term in one of the three classes, then there will be a large interference term in at least one of the other two classes. For example, for $|\sin(2\gamma)| \approx 1$ we get $|\sin(2\phi)| \gtrsim 0.7$ for either $\phi = \alpha$ or $\phi = \beta$. This turns out to have important bearings on the luminosity considerations presented in section 6.

6. Luminosity Considerations

We now proceed to apply the results of the last section to find the luminosity required to observe a statistically significant CP-violating asymmetry at an electron-positron B factory. We choose a “favorite” B^0 decay mode that corresponds to each of the three classes of asymmetry measurements, estimate the relevant experimental and detector-related numbers that are associated with each of these decays, and then combine them with the magnitude of the appropriate CP-violating interference term to estimate the luminosity required for a 3σ effect. One must always be aware that much of the experimental and detector-related input to these calculations is based on estimates or educated guesses; they may change with future data when specific branching ratios are *measured*, and other decay modes than we have chosen, or combinations of them, may well turn out to be optimal.

We limit our discussion to asymmetric machines running at the $\Upsilon(4S)$, and to polarized Z^0 machines. For each type of machine, we will quote two values of integrated luminosity, \mathcal{L}_u and \mathcal{L}_d , corresponding to the minimal and maximal magnitude of the interference term, $|\sin(2\phi)|$, respectively. An experiment which is capable of acquiring integrated luminosity above \mathcal{L}_u is guaranteed a statistically significant (3σ) CP-violating asymmetry in the Standard Model. On the other hand, an experiment with an integrated luminosity below \mathcal{L}_d is not expected to observe a CP-violating asymmetry. Thus, observation of an effect in the latter case would indicate a source outside the Standard Model, while if no significant asymmetry is observed it will not add to our knowledge of the Standard Model.

To compute the integrated luminosity needed to measure a CP-violating asymmetry to a given level of accuracy, we follow fairly closely the analysis and assump-

tions made in the Snowmass 88 report:²⁴ The formal expression for the integrated luminosity is:

$$\int \mathcal{L} dt = \{2\sigma(e^+e^- \rightarrow \bar{b}b) f_0 B \epsilon_r \epsilon_t [(1 - 2W) d \delta(\sin 2\phi)]^2\}^{-1} \quad (6.1)$$

where:

f_0 is the fraction of B^0 's in the b -quark fragmentation;

B is the product of the branching fractions to the desired final state f ;

ϵ_r is the reconstruction efficiency of the final state f ;

ϵ_t is the tagging efficiency, *i.e.* the fraction of events in which the flavor of the B which decays to f can be measured;

W is the fraction of incorrect tags;

d is a dilution factor which takes into account the loss in asymmetry due to fitting, time integration, and/or the mixing of the tagged decay;

$\delta(\sin 2\phi)$ is the required accuracy on the CP asymmetry parameter $\sin(2\phi)$, taken to be $|\sin(2\phi)/3|$ for a 3σ effect.²⁵

Table 2 lists the branching ratios and reconstruction efficiencies for the modes in each of the three different classes which we consider.

TABLE 2
Branching Ratios and Reconstruction Efficiencies for
Representative Decay Modes of the Three Classes

Class	Decay mode	B	ϵ_r (asym. $\Upsilon(4S)$)	ϵ_r (pol. Z^0)
(i)	$B_d \rightarrow \psi K_S$	$(3 \times 10^{-4}) \times 0.14$	0.61	0.46
(ii)	$B_d \rightarrow \pi^+\pi^-$	2×10^{-5}	0.8	0.8
(iii)	$B_s \rightarrow \rho K_S$	3×10^{-5}	—	0.46

The rate¹³ for the mode $B_d \rightarrow \psi K_S$ is a factor of 0.6 times that²⁴ used in the Snowmass 88 report. The modes $B_d \rightarrow \pi^+\pi^-$ and $B_s \rightarrow \rho K_S$ have yet to be observed, and estimates of their branching ratios depend on uncertain hadronic matrix elements and $|V_{ub}/V_{cb}|$. As working values, we use branching ratios of 2×10^{-5} for $B_d \rightarrow \pi^+\pi^-$ and 3×10^{-5} for $B_s \rightarrow \rho K_S$. The latter, in particular, might be thought optimistic, but, as will be seen shortly, even this branching ratio will not help to lower the required luminosities. The reconstruction efficiencies in Table 2 should be achievable, at least within a factor of two, by state-of-the-art detectors.²⁶ Table 3 summarizes the characteristics of B production and tagging at the two machines which are relevant to Eq. (6.1). Combinations of branching ratios and tagging efficiencies which are higher than given here will result in a lower required luminosity, and *vice versa*.

TABLE 3

Comparison between the Asymmetric $\Upsilon(4S)$ and the Polarized Z^0

Factor	Asymmetric $\Upsilon(4S)$	Polarized Z^0
$\sigma(e^+e^- \rightarrow \bar{b}b)$ (nb)	1.2	6.3
Fraction of B^0 , f_0	0.5 (for B_d)	0.35 (for B_d) 0.15 (for B_s)
Tag efficiency, ϵ_t	0.48	0.61
Wrong tag fraction, W	0.08	0.125
Asymmetry dilution, d	0.61 (for B_d)	0.61 (for B_d) 0.50 (for B_s)

6.1. ASYMMETRIC MACHINE OPERATING AT THE $\Upsilon(4S)$

We update the fraction of neutral B_d mesons at the $\Upsilon(4S)$ to be 0.5 (rather than the value 0.43 used at Snowmass 88) from the recent measurements by ARGUS and CLEO collaborations,²¹ and take the tagging efficiency to be 48% when the charges of both the kaons and the leptons from the accompanying B are used. The solid curves in Figure 9 show \mathcal{L}_u and \mathcal{L}_d for the class (i) process $B_d \rightarrow \psi K_S$ alone as a function of the top mass. To observe the smallest possible interference term, $|\sin(2\beta)|$, at the 3σ level, the required integrated luminosity is

$$\mathcal{L}_u \approx 4 \times 10^{41} \text{ cm}^{-2} \quad (6.2)$$

for $m_t \gtrsim 130$ GeV. It is lower for a lighter top. At the other extreme, if the interference term is maximal, then an integrated luminosity $\mathcal{L}_d \approx 2-3 \times 10^{39} \text{ cm}^{-2}$ will suffice.

An experiment which is sensitive to both class (i) and class (ii) processes would require a smaller integrated luminosity to see a statistically significant effect. In much the same way that we defined I_2 in the previous section, we define \mathcal{L}_{u2} and \mathcal{L}_{d2} by ranging over all allowed triangles²⁷ for a combination of the class (i) and class (ii) processes $B_d \rightarrow \psi K_S$ and $B_d \rightarrow \pi^+\pi^-$. Thus, \mathcal{L}_{u2} is the integrated luminosity which guarantees in the Standard Model an observation of a CP-violating asymmetry at the 3σ level, if asymmetries in both classes (i) and (ii) are measured. The dashed curves in Figure 9 show \mathcal{L}_{u2} and \mathcal{L}_{d2} as a function of the top mass. We find that

$$\mathcal{L}_{u2} \approx 3 \times 10^{41} \text{ cm}^{-2} \quad (6.3)$$

for $m_t \approx 130$ GeV. This is not much below the value of \mathcal{L}_u given previously.

\mathcal{L}_{u2} drops below 10^{41} cm^{-2} only if the top is lighter than 90 GeV or heavier than 200 GeV. If the values of the interference terms are favorable, an integrated luminosity of $\mathcal{L}_{d2} \approx 2 - 3 \times 10^{39}$ cm^{-2} will suffice, as was the case for class (i) processes alone.

The addition of class (ii) processes has not changed much. Could we have lower required luminosities if we simultaneously search for CP-violating asymmetries in all three classes? An e^+e^- collider could run at the $\Upsilon(5S)$ to study B_s decays which fall in class (iii). However, lower cross-section, lower tagging efficiencies and low hadronization of a b -quark into a B_s -meson make this possibility unattractive. We find that a simultaneous measurement of processes in all three classes does not lower the required luminosity.

6.2. POLARIZED Z^0

We consider a Z^0 machine with a 90% longitudinally polarized electron and/or positron beam. The tagging of B^0 versus \bar{B}^0 mesons can be done geometrically *via* the forward-backward asymmetry.²⁸ This, together with a large cross-section makes it an interesting alternative to the asymmetric $\Upsilon(4S)$ machine. Since a polarized Z^0 machine is automatically a source of B_s mesons, we consider situations where (1) the detector is sensitive to only class (i) processes, (2) the detector is sensitive to both class (i) and (ii) processes, and (3) the detector is sensitive to all three classes simultaneously.

The results for detection of only class (i) decays are shown in Figure 10, where \mathcal{L}_u and \mathcal{L}_d are presented as a function of the top mass. The results are smaller by a factor of 2.8 than those for the asymmetric $\Upsilon(4S)$ machine (see the analogous

Figure 9). A 90% polarized Z^0 machine needs

$$\mathcal{L}_u \approx 1.4 \times 10^{41} \text{ cm}^{-2} \quad (6.4)$$

in order to be guaranteed a 3σ CP-violating asymmetry in the mode $B_d \rightarrow \psi K_S$ within the Standard Model. The minimum luminosity to see a significant effect is $\mathcal{L}_d \approx 10^{39} \text{ cm}^{-2}$. While individually different, the ratio of required luminosities between the asymmetric $\Upsilon(4S)$ and polarized Z^0 machines is very close to that found in Ref. 24.

The luminosity required will be less if we are in situation (2). The argument follows exactly the same lines as for the $\Upsilon(4S)$ machine, and the results are shown in Figure 10 (compare to Figure 9). We find

$$\mathcal{L}_{u2} \approx 8 \times 10^{40} \text{ cm}^{-2} \quad (6.5)$$

for $m_t \approx 130 \text{ GeV}$. For either smaller or larger top masses, the required luminosity would be less, *e.g.*, $3 \times 10^{40} \text{ cm}^{-2}$ for $m_t \approx 200 \text{ GeV}$. The minimal luminosity for a useful experiment is still $\mathcal{L}_{d2} \approx 10^{39} \text{ cm}^{-2}$, as was the case for \mathcal{L}_d .

Could we do better if we include in addition the measurement of a class (iii) decay asymmetry? If we move to situation (3) above, then we need to range over all possible allowed unitarity triangles while considering the luminosity required to see a statistically significant asymmetry in $B_d \rightarrow \psi K_S$, $B_d \rightarrow \pi^+ \pi^-$, and $B_s \rightarrow \rho K_S$ decays within the Standard Model. In analogy to the previous situations, we define \mathcal{L}_{u3} and \mathcal{L}_{d3} to be the maximum and minimum integrated luminosity which is required to see a statistically significant asymmetry. The question that we asked above can be rephrased into: is \mathcal{L}_{u3} significantly smaller than \mathcal{L}_{u2} ? This could be

the case if the product $|\sin(2\phi)|^2 \cdot (f_0 B \epsilon_r \epsilon_t d^2)$ was larger for the $B_s \rightarrow \rho K_S$ mode than for the other two [see Eq. (6.1)]. The answer is given in Figure 10, where both \mathcal{L}_{u2} and \mathcal{L}_{u3} (as well as \mathcal{L}_{d2} and \mathcal{L}_{d3}) are displayed as the *same* dashed curve. As mentioned in section 5, there is no choice of CKM parameters which makes the CP-asymmetry in $B_s \rightarrow \rho K_S$ large while rendering the asymmetries in $B_d \rightarrow \psi K_S$ and $B_d \rightarrow \pi^+ \pi^-$ both small. Given our assumptions on production cross sections, branching ratios, and efficiencies, it follows that there is no improvement with a simultaneous measurement of asymmetries in three rather than two classes.

Our conclusions regarding the $B_s \rightarrow \rho K_S$ mode for the asymmetric $\Upsilon(4S)$ machine (operating for this purpose at the $\Upsilon(5S)$ resonance) and the polarized Z^0 machine do not imply that a measurement of class (*iii*) asymmetries is useless. On the contrary, this is a very important measurement that will provide additional information on the Standard Model parameters. Whether the independently-measured three angles will sum up to 180° is a stringent test for the CKM model of CP-violation. All we conclude here is that measuring CP-asymmetry in class (*iii*) processes in addition to class (*i*) and class (*ii*) asymmetries will not relax the luminosity requirements for the polarized Z^0 machine, and certainly not for the asymmetric $\Upsilon(4S)$ machine.

FIGURE CAPTIONS

- 1) Representation in the complex plane of the triangle formed (a) by the CKM matrix elements V_{ub}^* , $V_{cd} \cdot V_{cb}^*$, and V_{td} , and the rescaled triangle (b) with vertices at $A(\rho, \eta)$, $B(1, 0)$, and $C(0, 0)$. A relevant B^0 decay mode is indicated for the angle involved in the corresponding CP-violating asymmetry.
- 2) Constraints from $|V_{ub}/V_{cb}|$ (dotted circles), x_d (dashed circles), and ϵ (solid hyperbolas) on the rescaled unitarity triangle for $m_t = 80$ GeV. The shaded region is that allowed for the vertex $A(\rho, \eta)$. (a) $|V_{cb}| = 0.036$, (b) $|V_{cb}| = 0.046$, (c) $|V_{cb}| = 0.056$.
- 3) Constraints from $|V_{ub}/V_{cb}|$ (dotted circles), x_d (dashed circles), and ϵ (solid hyperbolas) on the rescaled unitarity triangle for $m_t = 120$ GeV. The shaded region is that allowed for the vertex $A(\rho, \eta)$. (a) $|V_{cb}| = 0.036$, (b) $|V_{cb}| = 0.046$, (c) $|V_{cb}| = 0.056$.
- 4) Constraints from $|V_{ub}/V_{cb}|$ (dotted circles), x_d (dashed circles), and ϵ (solid hyperbolas) on the rescaled unitarity triangle for $m_t = 160$ GeV. The shaded region is that allowed for the vertex $A(\rho, \eta)$. (a) $|V_{cb}| = 0.036$, (b) $|V_{cb}| = 0.046$, (c) $|V_{cb}| = 0.056$.
- 5) Constraints from $|V_{ub}/V_{cb}|$ (dotted circles), x_d (dashed circles), and ϵ (solid hyperbolas) on the rescaled unitarity triangle for $m_t = 200$ GeV. The shaded region is that allowed for the vertex $A(\rho, \eta)$. (a) $|V_{cb}| = 0.036$, (b) $|V_{cb}| = 0.046$, (c) $|V_{cb}| = 0.056$.
- 6) The upper and lower bounds on the angles α , β , and γ of the unitarity triangle as a function of m_t .
- 7) The upper and lower bounds (solid curves) for the interference term, $\text{Im } \lambda$, as

a function of m_t . The lower bound on $|\text{Im } \lambda|$, is shown as the dotted curve.

(a) $\text{Im } \lambda = -\sin(2\alpha)$, (b) $\text{Im } \lambda = -\sin(2\beta)$, (c) $\text{Im } \lambda = -\sin(2\gamma)$.

- 8) The quantities I_1 (solid curve), I_2 (dashed curve), and I_3 (dotted curve) as a function of m_t (see text).
- 9) The integrated luminosity of an asymmetric electron-positron collider operating at the $\Upsilon(4S)$ required to observe a statistically significant (3σ) CP-violating asymmetry as a function of m_t . Minimum and maximum required integrated luminosity when CP-violating asymmetries are searched for in the decay $B_d \rightarrow \psi K_S$ (solid curve), or simultaneously in the decays $B_d \rightarrow \psi K_S$ and $B_d \rightarrow \pi^+\pi^-$ (dashed curve). The minimum integrated luminosity curves in these two cases are identical.
- 10) The integrated luminosity of an electron-positron collider operating at the Z with a 90% polarized beam required to observe a statistically significant (3σ) CP-violating asymmetry as a function of m_t . Minimum and maximum required integrated luminosity when CP-violating asymmetries are searched for in the decay $B_d \rightarrow \psi K_S$ (solid curve), or simultaneously in the decays $B_d \rightarrow \psi K_S$ and $B_d \rightarrow \pi^+\pi^-$ (dashed curve). The dashed curves apply as well when CP-violating asymmetries in the three decays, $B_d \rightarrow \psi K_S$, $B_d \rightarrow \pi^+\pi^-$, and $B_s \rightarrow \rho K_S$ are simultaneously searched for.

REFERENCES

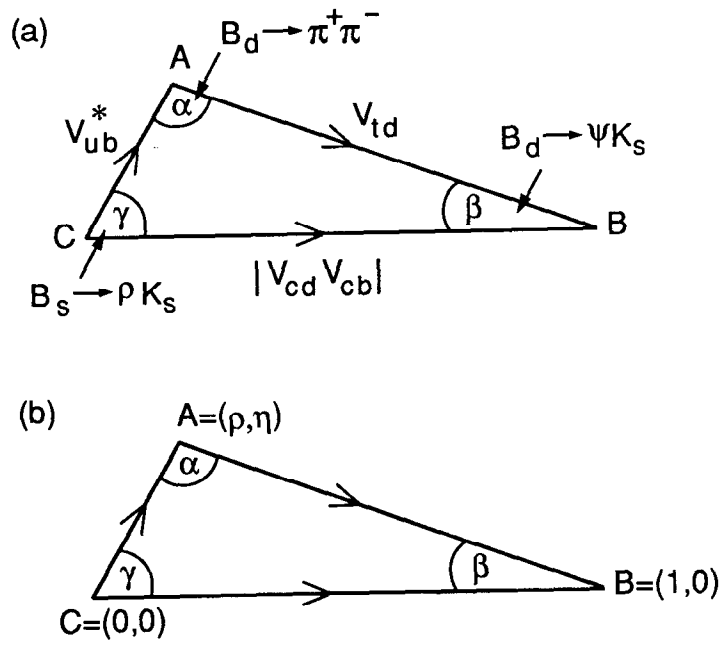
1. J. H. Christenson, J. W. Cronin, V. L. Fitch, and R. Turlay, *Phys. Rev. Lett.* **13**, 138 (1964).
2. K. J. Foley *et al.*, in *Proceedings of the Workshop on Experiments, Detectors, and Experimental Areas for the Supercollider*, Berkeley, July 7-17, 1987, edited by R. Donaldson and M. G. D. Gilchriese (World Scientific, Singapore, 1988), p. 701.
3. J. L. Rosner, A. I. Sanda, and M. P. Schmidt, in *Proceedings of the Workshop on High Sensitivity Beauty Physics at Fermilab*, Fermilab, November 11-14, 1987, edited by A. J. Slaughter, N. Lockyer, and M. Schmidt (Fermilab, Batavia, 1988), p. 165; C. Hamzaoui, J. L. Rosner and A. I. Sanda, in *Proceedings of the Workshop on High Sensitivity Beauty Physics at Fermilab*, Fermilab, November 11-14, 1987, edited by A. J. Slaughter, N. Lockyer, and M. Schmidt (Fermilab, Batavia, 1988), p. 215.
4. P. Krawczyk *et al.*, *Nucl. Phys.* **B307**, 19 (1988).
5. G. Belanger *et al.*, in *Proceedings of the 1988 Summer Study on High Energy Physics in the 1990s*, edited by S. Jensen (World Scientific, Singapore, 1989), p. 339.
6. L.-L. Chau and W.-Y. Keung, *Phys. Rev. Lett.* **53**, 1802 (1984); J. D. Bjorken, private communication and Fermilab preprint, 1988 (unpublished); C. Jarlskog and R. Stora, *Phys. Lett.* **208B**, 268 (1988); J. L. Rosner, A. I. Sanda, and M. P. Schmidt, Ref. 3; C. Hamzaoui, J. L. Rosner and A. I. Sanda, Ref. 3.
7. Particle Data Group, *Phys. Lett.* **204B**, 1 (1988).

8. J. D. Bjorken, private communication; J. L. Rosner, A. I. Sanda, and M. P. Schmidt, Ref. 3; C. Hamzaoui, J. L. Rosner and A. I. Sanda, Ref. 3; I. I. Bigi *et al.*, in *CP Violation*, edited by C. Jarlskog (World Scientific, Singapore, 1989), p. 175; A. E. Blinov, V. A. Khoze, and N. G. Uraltsev, *Int. J. Mod. Phys. A* 4, 1933 (1989); K. R. Schubert, Karlsruhe preprint IEKP-KA/88-4, 1988 (unpublished).
9. L. Wolfenstein, *Phys. Rev. Lett.* 51, 1945 (1983).
10. I. Dunietz and J. L. Rosner, *Phys. Rev. D* 34, 1404 (1986) and references therein.
11. I. Bigi and A. Sanda, *Nucl. Phys. B* 281, 41 (1987).
12. For the final states with an \bar{s} quark, the quark level process is assumed to be followed by $\bar{s} \leftrightarrow \bar{d}$ through $K^0 - \bar{K}^0$ mixing.
13. D. Kreinick, invited talk on results from the CLEO experiment, at the 1989 International Symposium on Lepton-Photon Interactions at High Energies, Stanford, August 6 - 12, 1989 (unpublished).
14. We thank S. Wagner for his comments on the possibility of using decay modes involving ω mesons.
15. M. Gronau, Max Planck Institute preprint MPI-PAE/PTh-27/89, 1989 (unpublished).
16. B. Grinstein, Fermilab preprint FERMILAB-PUB-89/158-T, 1989 (unpublished).
17. I. Bigi, private communication.
18. Y. Nir, *Nucl. Phys. B* 306, 14 (1988).

19. P. Sinervo, invited talk on CDF results on the search for the top quark, at the 1989 International Symposium on Lepton-Photon Interactions at High Energies, Stanford, August 6 - 12, 1989 (unpublished).
20. U. Amaldi *et al.*, Phys. Rev. D36, 1385 (1987); G. Costa *et al.*, Nucl. Phys. B297, 244 (1988).
21. M. Danilov and D. Kreinick, invited talks on results from the ARGUS and CLEO experiments, respectively, at the 1989 International Symposium on Lepton-Photon Interactions at High Energies, Stanford, August 6 - 12, 1989 (unpublished). We have taken the signal in both experiments for $b \rightarrow u$ transitions as implying, in a range of models, $|V_{ub}/V_{cb}| > 0.04$; and averaged the two results for $B^0 - \bar{B}^0$ mixing to obtain $r_d = 0.17 \pm 0.06$, and hence the result for x_d in the text. With a less conservative range, $r_d = 0.17 \pm 0.04$, our results for the luminosity requirements remain essentially unchanged.
22. This range is in agreement with that quoted by Ref. 4, but disagrees with that in Ref. 2 .
23. Here we disagree with both Ref. 2 and Ref. 4, who quote an upper limit on the magnitude of the interference term of 0.6 .
24. G. Feldman *et al.*, in *Proceedings of the 1988 Summer Study on High Energy Physics in the 1990s*, edited by S. Jensen (World Scientific, Singapore, 1989), p. 561.
25. For large values of $|\sin(2\phi)|$ the calculation of a 3σ effect has to be modified. We neglect this correction here.
26. We thank P. Burchat, D. Cords, N. Roe, and S. Wagner for discussions on detector efficiencies that can be envisaged for various decay modes.

27. For each triangle we define $\mathcal{L}_2(\Delta) \equiv \min\{\int dt\mathcal{L}(B_d \rightarrow \psi K_S), \int dt\mathcal{L}(B_d \rightarrow \pi^+\pi^-)\}$, where $\int dt\mathcal{L}(B_d \rightarrow f)$ is the integrated luminosity needed to observe a 3σ asymmetry in the decay $B_d \rightarrow f$. \mathcal{L}_{u2} and \mathcal{L}_{d2} are then the maximum and minimum, respectively, of this quantity obtained in ranging over all allowed triangles. \mathcal{L}_{u2} and I_2 do not necessarily correspond to the same set of values for the CKM parameters.

28. W. B. Atwood, I. Dunietz, and P. Grosse-Wiesmann, Phys. Lett. B216, 227 (1989).



9-89

6466A1

Fig. 1

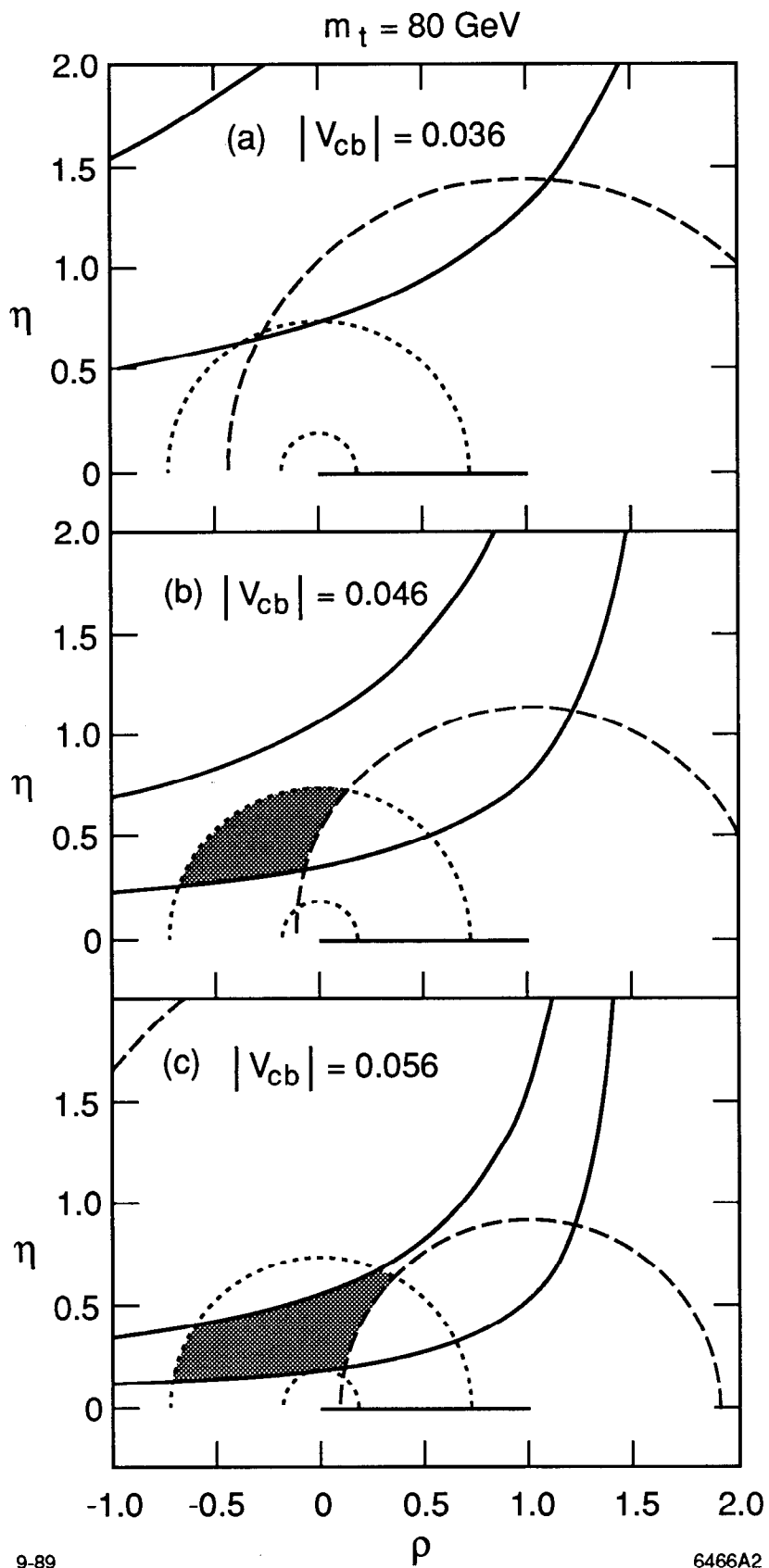


Fig. 2

$m_t = 120 \text{ GeV}$

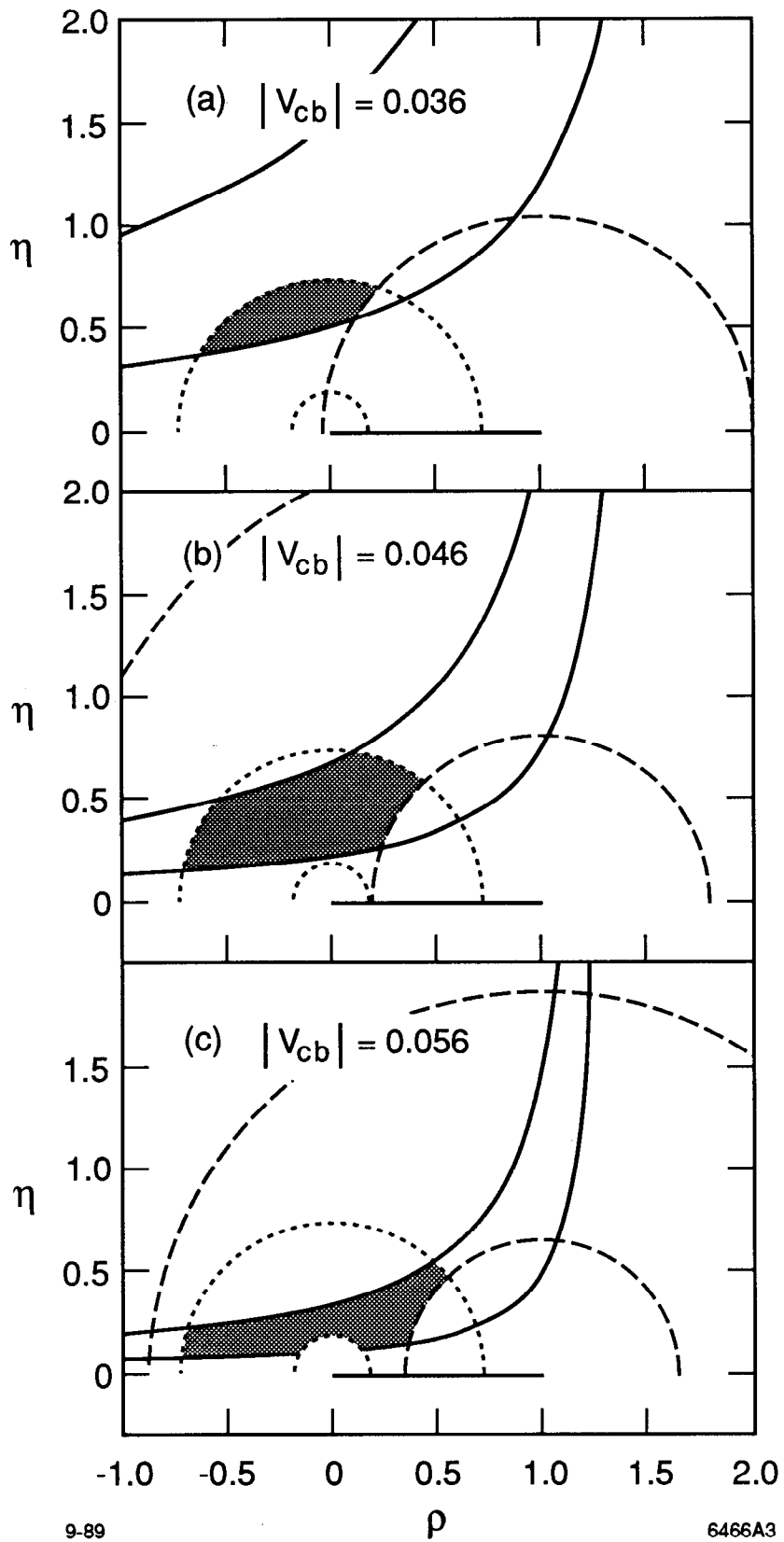


Fig. 3

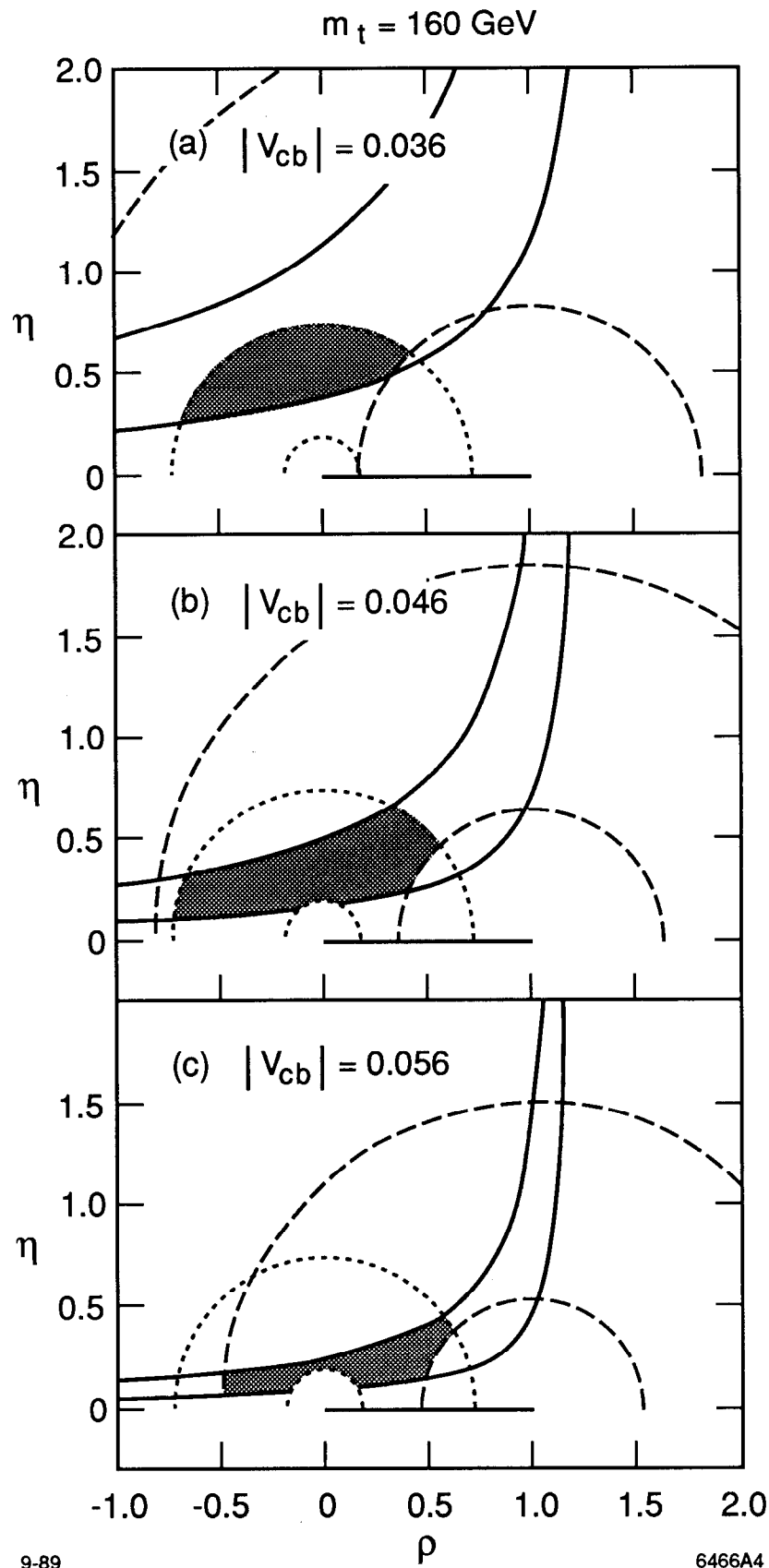


Fig. 4

$m_t = 200 \text{ GeV}$

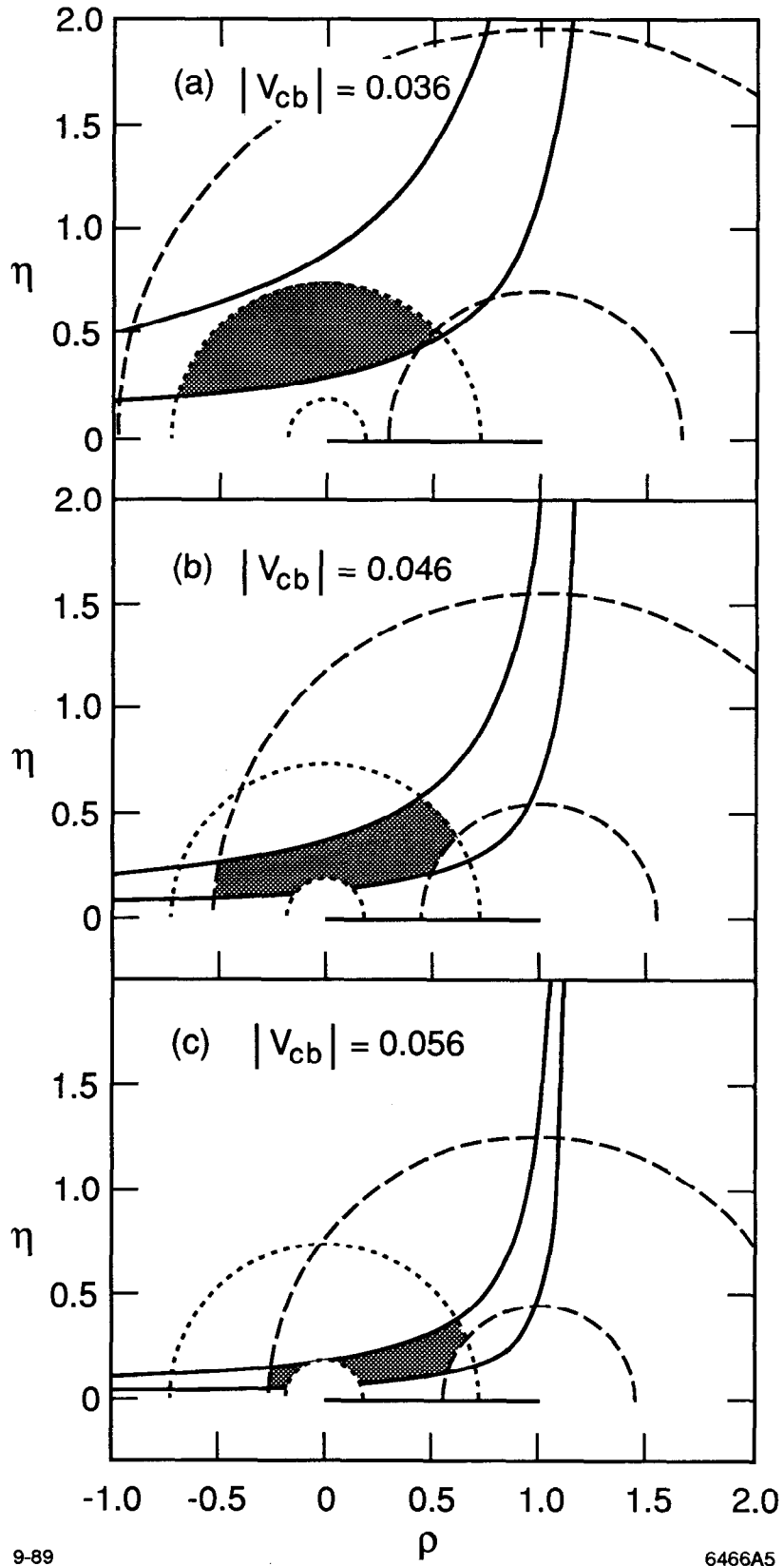


Fig. 5

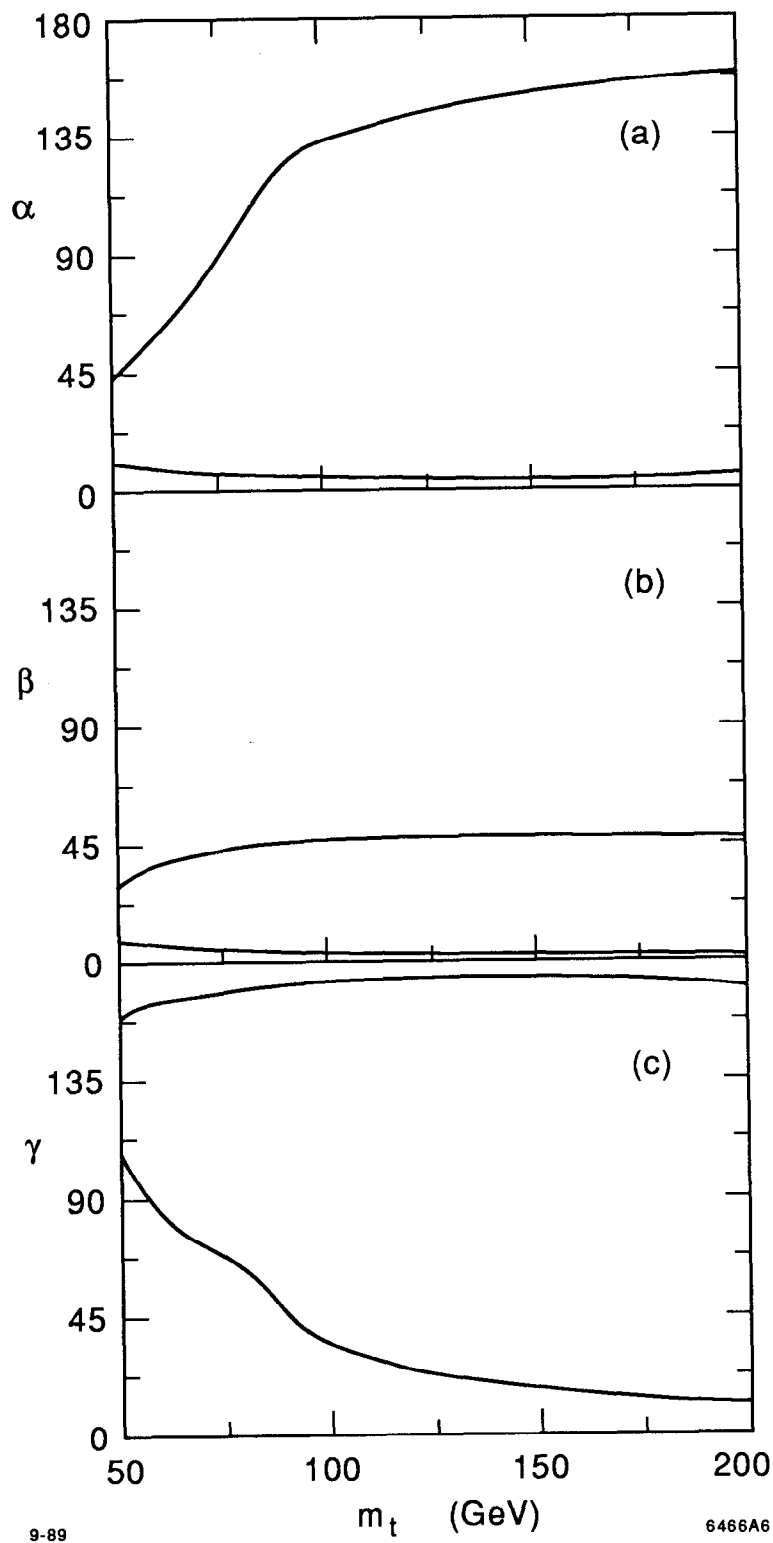


Fig. 6

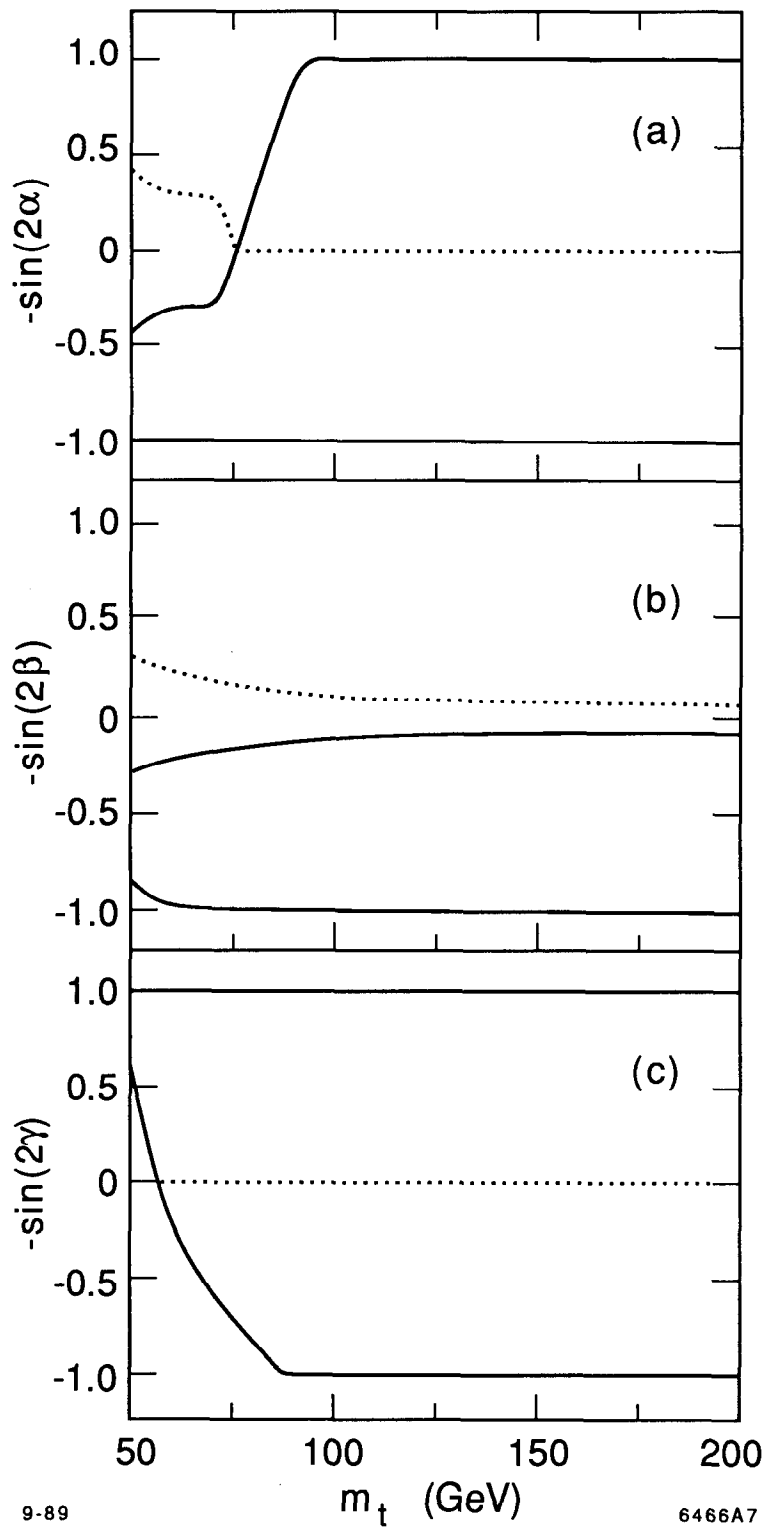
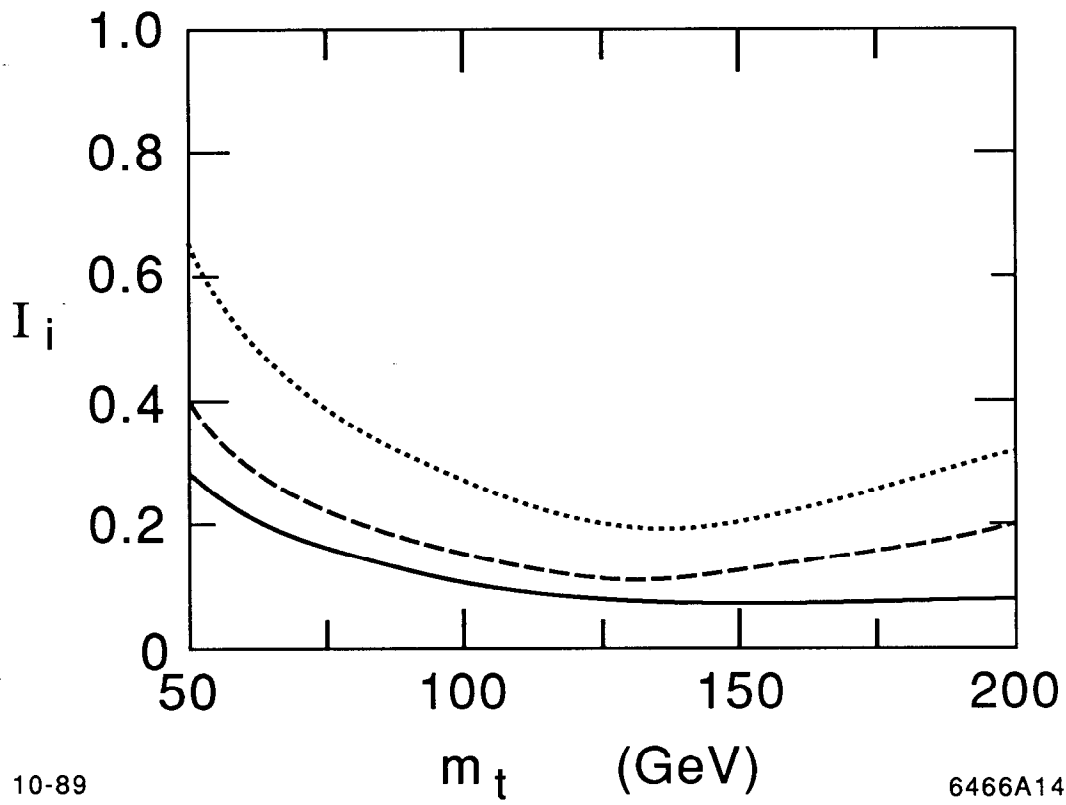


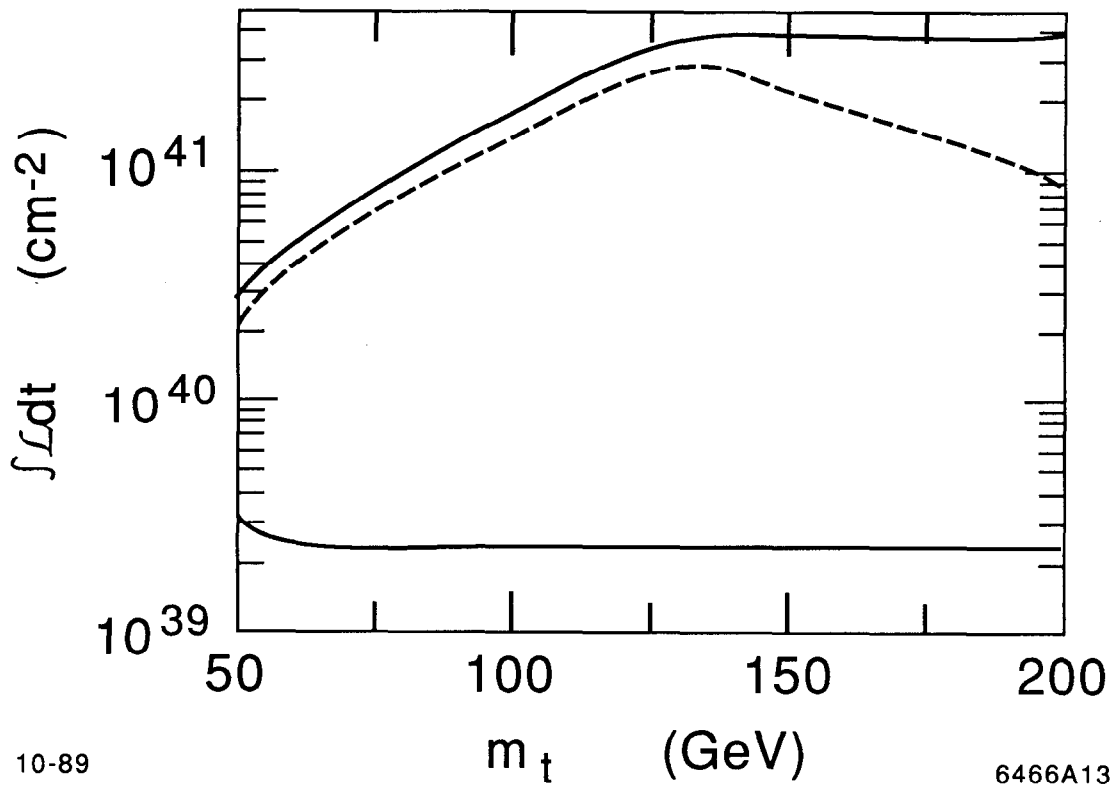
Fig. 7



10-89

6466A14

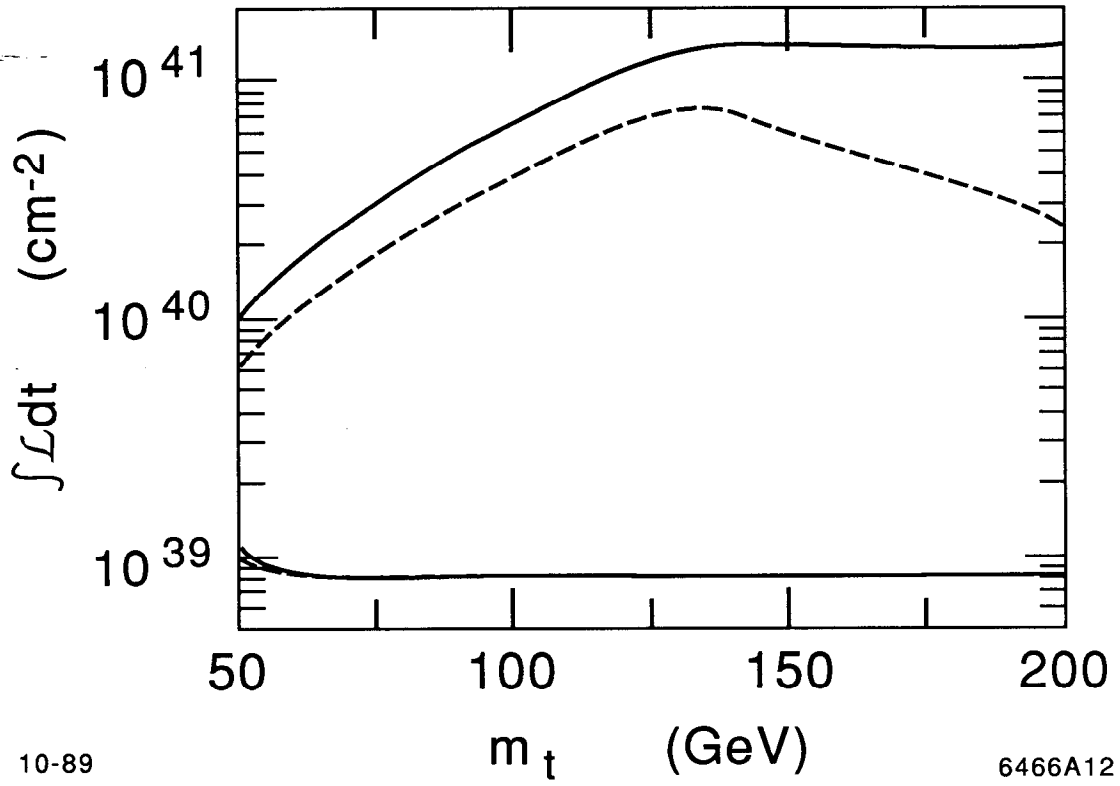
Fig. 8



10-89

6466A13

Fig. 9



10-89

6466A12

Fig. 10